Acta Crystallographica Section F
Structural Biology and Crystallization Communications
ISSN 1744-3091

Crystallization and preliminary characterization of chloromuconolactone dehalogenase from *Rhodococcus opacus* 1CP

Christian Roth,[a] Stefan R. Kaschabek,[b] Janosch A. D. Gröning,[b] Thomas Handrek,[b] Michael Schlömann[b] and Norbert Sträter[a]*

[a]Center for Biotechnology and Biomedicine, Institute of Bioanalytical Chemistry, Faculty of Chemistry and Mineralogy, University of Leipzig, Deutscher Platz 5, 04103 Leipzig, Germany, and [b]Interdisciplinary Ecological Center, TU Bergakademie Freiberg, Leipziger Strasse 29, 09599 Freiberg, Germany

Correspondence e-mail: strater@bbz.uni-leipzig.de

Received 12 January 2012
Accepted 19 March 2012

Chloroaromatic compounds are often very persistent environmental pollutants. Nevertheless, numerous bacteria are able to metabolize these compounds and to utilize them as sole energy and carbon sources. *Rhodococcus opacus* 1CP is able to degrade several chloroaromatic compounds, some of them *via* a variation of the 3-chlorocatechol branch of the modified *ortho*-cleavage pathway. This branch in *R. opacus* differs from that in *Proteobacteria* in the inability of the chloromuconate cycloisomerase to dehalogenate. Instead, a unique enzyme designated as chloromuconolactone dehalogenase (ClcF) is recruited. ClcF dehalogenates 5-chloromuconolactone to *cis*-dienelactone and shows a high similarity to muconolactone isomerases (EC 5.3.3.4). However, unlike the latter enzymes, it is unable to catalyse the isomerization of muconolactone to 3-oxoadipate enollactone. In order to characterize the catalytic mechanism of this unusual dehalogenase, the enzyme was crystallized and subjected to X-ray structural analysis. Data sets to up to 1.65 Å resolution were collected from two different crystal forms using synchrotron radiation. Crystal form I (space group $P2_1$) contained 40 subunits in the asymmetric unit, whereas ten subunits were present in crystal form II (space group $P2_12_12_1$). The self-rotation function revealed the orientations of the molecular symmetry axes of the homodecamer of 52 symmetry.

1. Introduction

Halogenated aromatic compounds are widespread in nature, for example in marine sponges and plants or as secondary metabolites in fungi or bacteria (Gribble, 2003). Furthermore, over several decades significant amounts of these compounds originating from anthropogenic sources, for example herbicides, organic solvents, chemical building blocks and pharmaceuticals, have been released into the environment (Reineke & Knackmuss, 1988; Chaudhry & Chapalamadugu, 1991; Häggblom, 1992). The presence of a Cl atom often drastically alters the physicochemical properties of an organic compound. In particular, many chloroaromatic compounds show considerable toxicity and tend to persist in the enviroment (Safe, 2005). During evolutionary adaptation, bacteria and some fungi have developed several catabolic mechanisms to degrade these substances. The most common and best characterized pathway, the modified *ortho*-pathway, is predominantly found in soil bacteria (Harwood & Parales, 1996). In this degradation route, a large number of chloroaromatics are funnelled into a few chlorocatechol isomers after initial degradation. Specialized enzymes comprising a chlorocatechol dioxygenase, a chloromuconate cycloisomerase, a dienelactone hydrolase and a maleylacetate reductase are responsible for the downstream processing of the isomers (Reineke & Knackmuss, 1988; Häggblom, 1992; Schlömann, 1994). The genes of the pathway may be exchanged between different species by catabolic plasmids and/or by transposable elements (Reineke & Knackmuss, 1988; Schlömann, 1994; van der Meer, 1997; Ravatn *et al.*, 1998). Recent biochemical and genetic studies of 3-chlorocatechol degradation by the Gram-positive actinobacterium *Rhodococcus opacus* 1CP revealed remarkable differences from known pathways in *Proteobacteria* (Eulberg *et al.*, 1998). The cycloisomerase in this pathway is not able to dehalogenate the cycloisomerized product 5-chloromuconolactone to a dienelactone. Therefore, strain 1CP expresses an additional chloro-

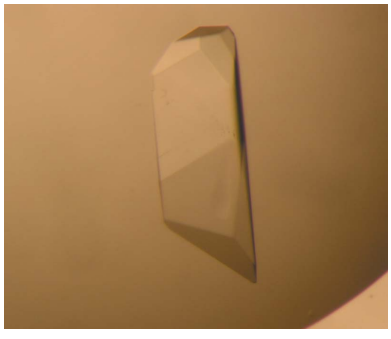

muconolactone dehalogenase (ClcF) to catalyse the conversion of 5-chloromuconolactone to *cis*-dienelactone, the substrate of the dienelactone hydrolase in this pathway (Fig. 1; Moiseeva *et al.*, 2002). The dehalogenase comprises 94 amino acids, with a corresponding molecular weight of 11.2 kDa. A high similarity is found to the muconolactone isomerases (MLIases), which catalyse the isomerization of muconolactone to 3-oxoadipate enollactone in the regular *ortho*-pathway of catechol, clearly indicating a relationship to these enzymes (Fig. 2). However, ClcF shows no activity towards muconolactone, whereas the muconolactone isomerases are able to isomerize muconolactone as well as to dehalogenate 5-chloromuconolactone, indicating a considerable extent of specialization (Prucha *et al.*, 1996; Moiseeva *et al.*, 2002). ClcF shares 49% sequence identity with the *Pseudomonas putida* PRS2000 muconolactone isomerase, for which a crystal structure has been determined to 3.3 Å resolution (PDB entry 1mli; Katti *et al.*, 1989). As a result of the limited resolution, only the C_α coordinates have been deposited in the Protein Data Bank. Despite a tremendous knowledge of their genetic organization and biochemical function, little is known about the structure and catalytic mechanism of these enzymes. We crystallized ClcF in two different crystal forms and collected data sets to 1.65 Å resolution. It is hoped that the structure will provide detailed knowledge about the structural ensemble and the catalytic mechanism of this class of enzymes. Moreover, it might allow identification of the changes in the protein sequence and structure which are responsible for the high specialization of the enzyme towards 5-chloromuconolactone.

2. Material and methods

2.1. Cloning, overexpression and purification

The *clcF* gene of *R. opacus* (GenBank accession No. AJ439407) was cloned in pET11a to obtain native protein. The protein was expressed in *Escherichia coli* BL21-CodonPlus (DE3)-RIL cells and purified to homogenity (Gröning *et al.*, unpublished work). Briefly, *E. coli* Bl21-CodonPlus (DE3)-RIL cells grown in 1 l LB medium were induced with 0.1 m*M* IPTG at an OD of 0.6–0.7 and incubated for a further 4 h at 303 K. The cells were harvested by centrifugation at 4000*g* for 20 min. The resulting cell pellet was resuspended in 25 m*M* Tris–HCl pH 7.5 and lysed by passing the suspension through a French press (Thermo Scientific) at 10.3 MPa. The cell debris was removed by centrifugation at 100 000*g* for 45 min. The resulting supernatant was heated to 338 K for 10 min and then rapidly cooled to 277 K. The precipitated protein was removed by centrifugation at 100 000*g* for 10 min and the supernatant was applied onto a HiTrap

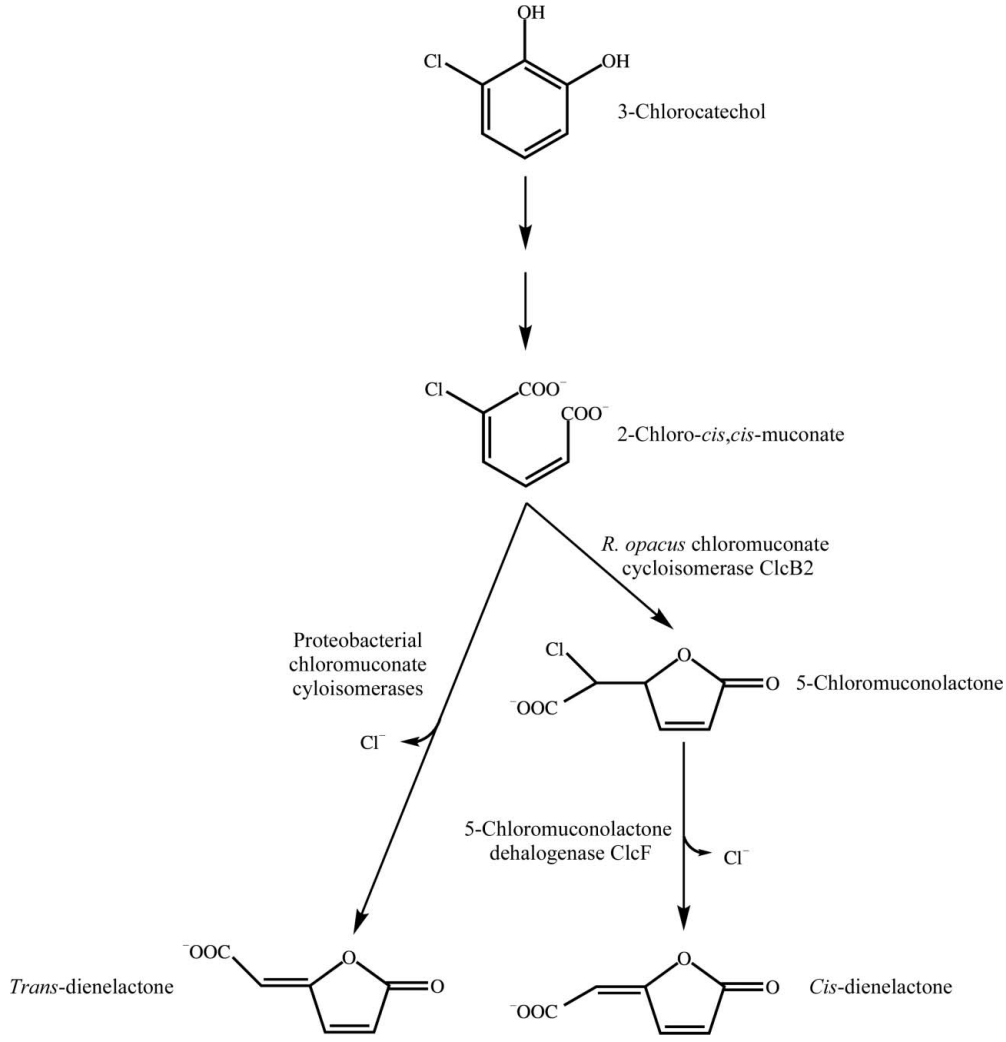

Figure 1
Differences in the modified *ortho*-pathway of *Proteobacteria* (left) and *R. opacus* 1CP (right). In *Proteobacteria* the cycloisomerase is able to dehalogenate the halogenated muconate, leading to a dienelactone, whereas the *R. opacus* cycloisomerase is not and ClcF has to complete the route, leading to *cis*-dienelactone.

Table 1
Data-collection and reduction statistics.

Values in parentheses are for the highest resolution shell.

Crystal form	I	II
X-ray source	BESSY MX 14.2	BESSY MX 14.2
Wavelength (Å)	0.91841	0.91841
Space group	$P2_1$	$P2_12_12_1$
Resolution (Å)	19.9–2.10 (2.21–2.10)	19.8–1.65 (1.74–1.65)
Unit-cell parameters		
a (Å)	151.1	78.2
b (Å)	79.4	103.6
c (Å)	198.8	141.7
β (°)	93.4	
Solvent content (%)	53.7	52.0
Molecules per asymmetric unit	40	10
Total reflections	869694	794928
Unique reflections	261677	138198
$\langle I/\sigma(I)\rangle$	18.2 (6.70)	19.3 (2.64)
Completeness (%)	95.3 (90.0)	99.6 (98.6)
$R_{\rm merge}$†	0.045 (0.183)	0.054 (0.508)
$R_{\rm meas}$‡	0.053 (0.216)	0.059 (0.586)
$R_{\rm p.i.m.}$§	0.029 (0.114)	0.023 (0.303)

† $R_{\rm merge} = \sum_{hkl}\sum_i |I_i(hkl) - \langle I(hkl)\rangle|/\sum_{hkl}\sum_i I_i(hkl)$. ‡ $R_{\rm meas} = \sum_{hkl}\{N(hkl)/[N(hkl)-1]\}^{1/2}\sum_i |I_i(hkl) - \langle I(hkl)\rangle|/\sum_{hkl}\sum_i I_i(hkl)$ (Diederichs & Karplus, 1997). § $R_{\rm p.i.m.} = \sum_{hkl}\{1/[N(hkl)-1]\}^{1/2}\sum_i |I_i(hkl) - \langle I(hkl)\rangle|/\sum_{hkl}\sum_i I_i(hkl)$ (Weiss, 2001).

Q-Sepharose column (GE Healthcare). The ClcF-containing fraction was supplemented with ammonium sulfate to a final concentration of 1.6 *M* and applied onto a HiTrap Phenyl Sepharose column (GE Healthcare). ClcF was eluted with a gradient from 1.6 to 0 *M* ammonium sulfate. The protein was then dialyzed against 25 m*M* Tris–HCl pH 7.5 and concentrated to 10 mg ml^{-1} using a Vivaspin-6 concentrator with a molecular-weight cutoff of 10 kDa. Aliquots of the concentrated protein were frozen in liquid nitrogen and stored at 193 K. The purity of the enzyme was verified by SDS–PAGE (Laemmli, 1970). Prior to crystallization, dynamic light scattering was carried out using a Spectroscatter 201 with laser light at 682 nm (Rina GmbH). The narrow single peak indicated monodispersity of the sample.

2.2. Crystallization

Initial crystallization conditions were found using in-house custom-made crystallization screens similar to the commercially available sparse-matrix and grid screens from Hampton Research and Jena Bioscience. Crystallization setups were performed by mixing equal amounts of protein and reservoir solution in a 96-well CrystalQuick plate (Greiner Bio-One). Plates were stored at 292 K and examined after defined time periods for the appearance of crystals. Optimization of the hits were carried out in 24-well crystallization plates using the hanging-drop vapour-diffusion method by mixing protein and reservoir solutions in an equal ratio to give a total drop volume of 2 µl. The best crystals used for data collection grew in 0.1 *M* MES pH 5.5–6.5, 1 *M* LiCl, 5–10% PEG 6000 (crystal form I) and 0.1 *M* bis-Tris pH 6.5–7.0, 0.4 *M* $MgCl_2$, 11–15% PEG 3350 (crystal form II) (Fig. 3).

2.3. Data collection and processing

For data collection, the crystals were transferred into a cryoprotectant solution containing all of the components of the mother liquor with a 2% higher concentration of the corresponding PEG and 25% ethylene glycol. The whole crystallization drop was exchanged for the cryoprotectant and crystals equilibrated with cryoprotectant were picked up with a nylon fibre loop (Hampton Research) and plunged into liquid nitrogen prior to data collection. Data were collected on a Rayonix MX 225 detector at 100 K using a synchrotron as a radiation source (Table 1). Rotation angles of 0.5° and 0.8° were chosen for crystal forms I and II, respectively. Although a relatively small oscillation angle of 0.5° was used for crystal form I, a high-resolution data cutoff of 2.1 Å had to be applied since the overlap of reflections at higher Bragg angles resulting from an unfavourable crystal orientation caused a loss of data completeness. Data sets for crystal form I were indexed and integrated using *iMOSFLM* (Battye *et al.*, 2011) and scaling was carried out using *SCALA* (Evans, 2006). For crystal form II the *XDS* software package was used (Kabsch, 2010). The protein content of the asymmetric unit was calculated using *MATTHEWS_COEF* from the *CCP*4 software package (Matthews, 1968; Winn *et al.*, 2011). The self-rotation function was calculated and plotted using *GLRF* (Tong & Rossmann, 1997). A resolution range of 15–3 Å and an integration radius of 15 Å were chosen for the calculation. Minimal contour levels of 4σ and 0.75σ were chosen for the 72° and 180° sections, respectively. The maximum contour level was set to 10σ and 8σ for the plots at 72° and 180°, respectively. A native Patterson map was calculated using *FFT* (Winn *et al.*, 2011).

3. Results and discussion

The chloromuconolactone dehalogenase was purified and concentrated to 10 mg ml^{-1} in 25 m*M* Tris–HCl pH 7.5. Aliquots of the frozen protein were thawed on ice and centrifuged at 16 000*g* for 2 min prior to use. Further storage at 277 K led to the formation of microcrystalline precipitate within 1 d. Therefore, the aliquots were centrifuged at 16 000*g* for 2 min prior to drop setup. Two crystallization conditions were identified in the crystallization screens with PEG 3350 and PEG 6000 as precipitants. Two crystal forms belonging

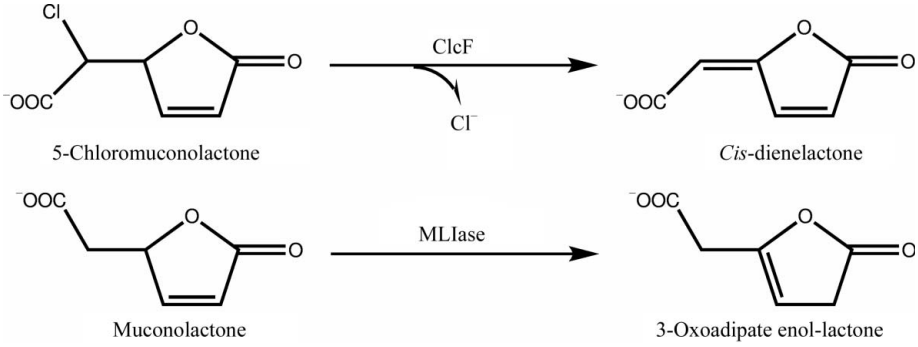

Figure 2
Comparison of the reactions catalysed by ClcF and MLIases. ClcF catalyzes the elimination of chloride ions with the formation of a double bond and no isomerization takes place. In contrast, MLIases isomerize a double bond and are able to dehalogenate 5-chloromuconolactone.

to space groups $P2_1$ and $P2_12_12_1$ were found (Table 1). Size-exclusion chromatography (Fig. 4) indicated that ClcF may form homodecamers, as also described for *P. putida* PRS2000 isomerase (Katti *et al.*, 1989). Based on the Matthews coefficient of 2.65 Å^3 Da^{-1} obtained using the monomer weight of 11 194 Da, four decamers are likely to be present in the asymmetric unit of crystal form I. With a Matthews cofficient of 2.56 Å^3 Da^{-1}, one decamer was expected in crystal form II. Therefore, we calculated a self-rotation function to verify the oligomeric state in the crystal and to determine the orientation of the oligomer. Fig. 5 shows the sections at 72° and 180° for crystal form II. The section at 72° shows two peaks corresponding to fivefold noncrystallographic symmetry axes. The axes are tilted by 33° relative to the crystallographic 2_1 axis along *c* in the *bc* plane. The section at 180° shows 20 peaks for local twofold axes, probably generated by two different orientations of the decamers in the unit cell. These peaks are located on a line that agrees with the tilting angle of the fivefold axis. Two of these peaks coincide with peaks

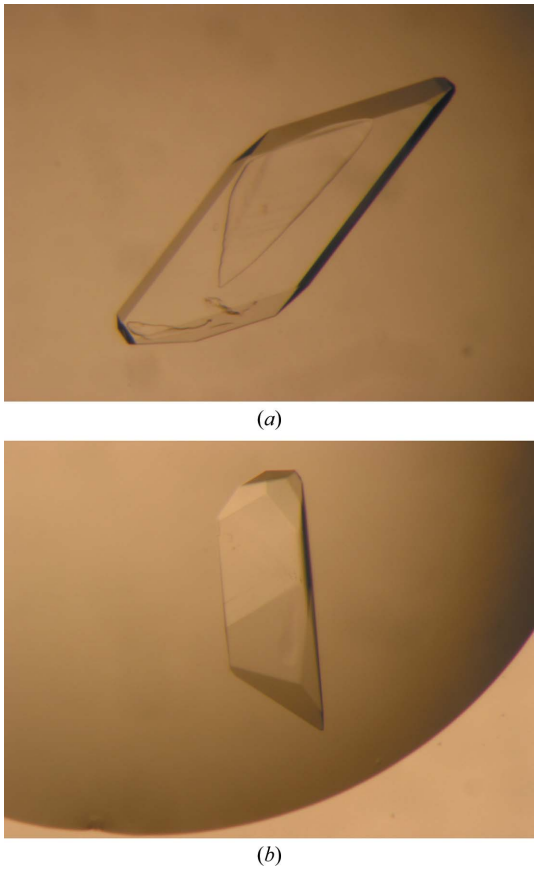

(*a*)

(*b*)

Figure 3
Crystals of ClcF belonging to crystal form I (*a*) with dimensions of 580 × 180 × 60 µm and crystal form II (*b*) with dimensions of 370 × 130 × 100 µm.

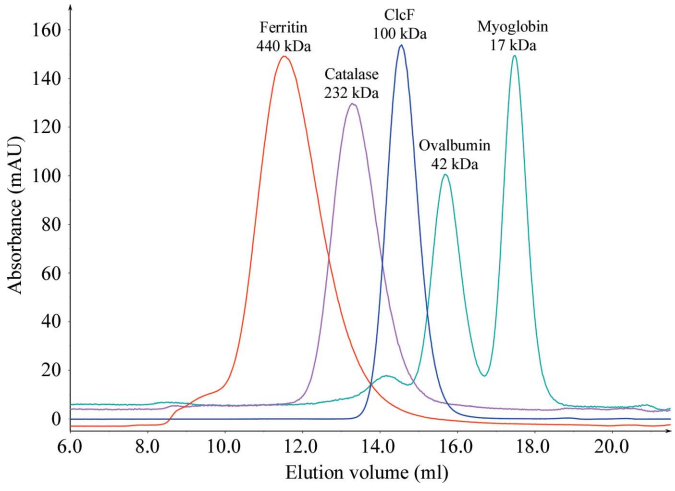

Figure 4
Chromatogram of gel filtration of ClcF and marker proteins for determination of the oligomeric state in solution. The running buffer consisted of 25 m*M* Tris pH 7.5, 250 m*M* NaCl.

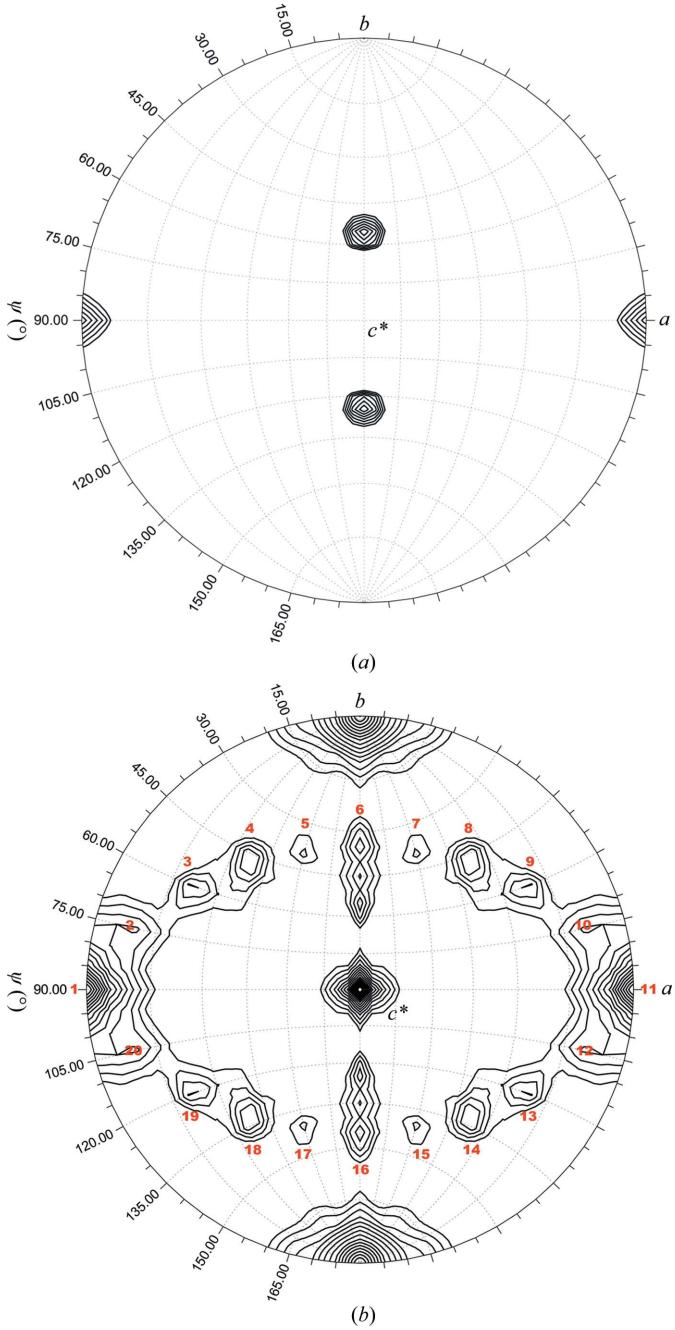

Figure 5
Self-rotation functions calculated using *GLRF* (Tong & Rossmann, 1997) at $\kappa = 72°$ (*a*) and $\kappa = 180°$ (*b*). Two distinct peaks in the 72° section reveal that the fivefold axes are tilted by 33° relative to the *c* axis. In the 180° section 20 peaks are generated by the twofold NCS axes of the decamers. The threshold contour level was set to 4σ in (*a*) and 0.75σ in (*b*).

resulting from the crystallographic 2_1 axis along *a*. The peaks are spaced every 18°. For a single decamer of 52 symmetry, a spacing of 36° is expected. This finding indicates that four decamers are present in the unit cell as two pairs with parallel fivefold axes. For each pair, the orientation differs by a rotation of 18° along the molecular fivefold axes. Translational NCS could not be detected in the native Patterson map. Molecular-replacement trials with *MOLREP* (Vagin & Teplyakov, 2010; Winn *et al.*, 2011) in crystal form II using a poly-Ala model of a monomer of *P. putida* PRS2000 isomerase showed ten peaks of roughly the same signal height in the rotation function. Taken together, these findings indicate that ClcF forms a decamer of 52 molecular symmetry. It is likely that the phase problem can be solved by molecular replacement utilizing the high noncrystallographic symmetry for phase refinement.

We thank Antje Keim for her help in crystallization. The authors thank Uwe Müller and his team for assistance during data collection at the HZB-MX beamlines at the Helmholtz-Zentrum Berlin. The Helmholtz-Zentrum Berlin is acknowledged for travel support.

References

Battye, T. G. G., Kontogiannis, L., Johnson, O., Powell, H. R. & Leslie, A. G. W. (2011). *Acta Cryst.* D**67**, 271–281.
Chaudhry, G. R. & Chapalamadugu, S. (1991). *Microbiol. Rev.* **55**, 59–79.
Diederichs, K. & Karplus, P. A. (1997). *Nature Struct. Biol.* **4**, 269–275.
Eulberg, D., Kourbatova, E. M., Golovleva, L. A. & Schlömann, M. (1998). *J. Bacteriol.* **180**, 1082–1094.
Evans, P. (2006). *Acta Cryst.* D**62**, 72–82.
Gribble, G. W. (2003). *Chemosphere*, **52**, 289–297.
Harwood, C. S. & Parales, R. E. (1996). *Annu. Rev. Microbiol.* **50**, 553–590.
Häggblom, M. M. (1992). *FEMS Microbiol. Rev.* **9**, 29–71.
Kabsch, W. (2010). *Acta Cryst.* D**66**, 125–132.
Katti, S. K., Katz, B. A. & Wyckoff, H. W. (1989). *J. Mol. Biol.* **205**, 557–571.
Laemmli, U. K. (1970). *Nature (London)*, **227**, 680–685.
Matthews, B. W. (1968). *J. Mol. Biol.* **33**, 491–497.
Meer, J. R. van der (1997). *Antonie Van Leeuwenhoek*, **71**, 159–178.
Moiseeva, O. V., Solyanikova, I. P., Kaschabek, S. R., Gröning, J., Thiel, M., Golovleva, L. A. & Schlömann, M. (2002). *J. Bacteriol.* **184**, 5282–5292.
Prucha, M., Peterseim, A., Timmis, K. N. & Pieper, D. H. (1996). *Eur. J. Biochem.* **237**, 350–356.
Ravatn, R., Studer, S., Springael, D., Zehnder, A. J. & van der Meer, J. R. (1998). *J. Bacteriol.* **180**, 4360–4369.
Reineke, W. & Knackmuss, H. J. (1988). *Annu. Rev. Microbiol.* **42**, 263–287.
Safe, S. H. (2005). *Chlorocarbons and Chlorohydrocarbons, Toxic Aromatics. Kirk–Othmer Encyclopedia of Chemical Technology*, 5th ed., Vol. 13. New York: Wiley.
Schlömann, M. (1994). *Biodegradation*, **5**, 301–321.
Tong, L. & Rossmann, M. G. (1997). *Methods Enzymol.* **276**, 594–611.
Vagin, A. & Teplyakov, A. (2010). *Acta Cryst.* D**66**, 22–25.
Weiss, M. S. (2001). *J. Appl. Cryst.* **34**, 130–135.
Winn, M. D. *et al.* (2011). *Acta Cryst.* D**67**, 235–242.